

## Radiation Heating in Selected NERVA\* Engine Components\*\*

J. C. Courtney+, N. A. Hertelendy+, B. A. Lindsey+  
Aerojet Nuclear Systems Company  
Sacramento, California

The role of heating from nuclear radiation in design of the NERVA\* engine is treated. Generally, radiation heating is more restrictive in design than material degradation considerations. Some components are subjected to very high gamma heating rates in excess of  $0.5 \text{ Btu/in}^3\text{-sec}$  in steel in the primary nozzle or  $0.25 \text{ Btu/in}^3\text{-sec}$  in aluminum in the pressure vessel. These components must be cooled by a fraction of the liquid hydrogen propellant before it is passed through the core, heated, and expanded out the nozzle as a gas. Other components that are subjected to lower heating rates such as the thrust structure and the disk shield are designed so that they would not require liquid hydrogen cooling. Typical gamma and neutron heating rates, resulting temperatures, and their design consequences are covered in this paper. The calculational techniques used in the nuclear and thermal analyses of the NERVA engine are briefly treated.

Most components in the NERVA engine (shown in Figure 1) must be designed to perform with high reliability in severe radiation environments. Radiation heating in several key components will be considered in this paper.

Generally, radiation heating is more restrictive in design than material degradation, due to the choice of material for each component.<sup>1</sup> The NERVA engine uses a relatively small core with a very high leakage fraction for both neutron and gamma radiation. At full power operation (75,000 lbs thrust and 1515 Mw reactor power), radiation-induced heating may exceed  $0.5 \text{ BTU/in}^3\text{-sec}$  in parts of the stainless steel nozzle, and may exceed  $0.2 \text{ BTU/in}^3\text{-sec}$  in the aluminum pressure vessel. Heating rates of this magnitude require that components be cooled by the liquid hydrogen propellant before it is passed through the core, heated, and expanded out the nozzle as a gas.

As long as the component is part of the propellant feed system or the pressure vessel and reactor assembly, liquid or gaseous hydrogen is

\*The Nuclear Engine for Rocket Vehicle Application (NERVA) program is administered by the Space Nuclear Systems Office, a joint office of the USAEC and NASA. Aerojet Nuclear Systems Company is prime contractor for the engine system and Westinghouse Electric Corporation is principal subcontractor responsible for the nuclear subsystem.

+Staff Members, Nuclear Science Section, Aerojet Nuclear Systems Company.

\*\*Public Release Approval: PRA/SA - SNPO-C, dated 24 November 1970.

available as a heat transfer agent. However, it is desirable that some components be designed so that they require no coolant, and thus do not influence the design of the propellant feed system. For example, the thrust structure is to be designed as an uncooled system. If a disk shield is required for some manned missions, it should be designed to operate without cooling. The thrust structure and the disk shield are located forward of the pressure vessel dome and are partially protected by a shadow shield inside the pressure vessel. Many other components forward of the dome, such as lines and valves, are already part of the liquid hydrogen propellant feed system and receive coolant during normal operation.

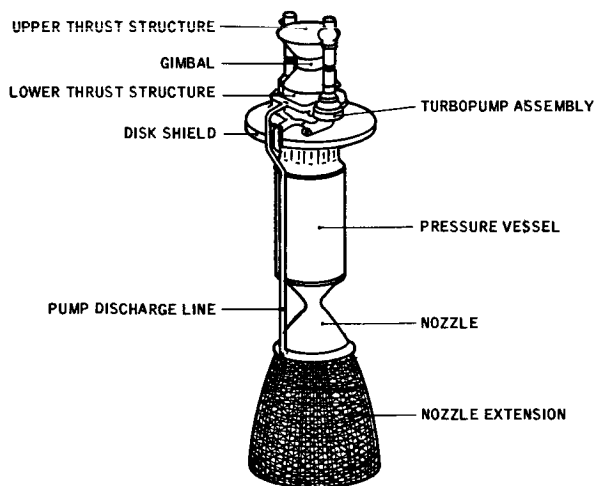
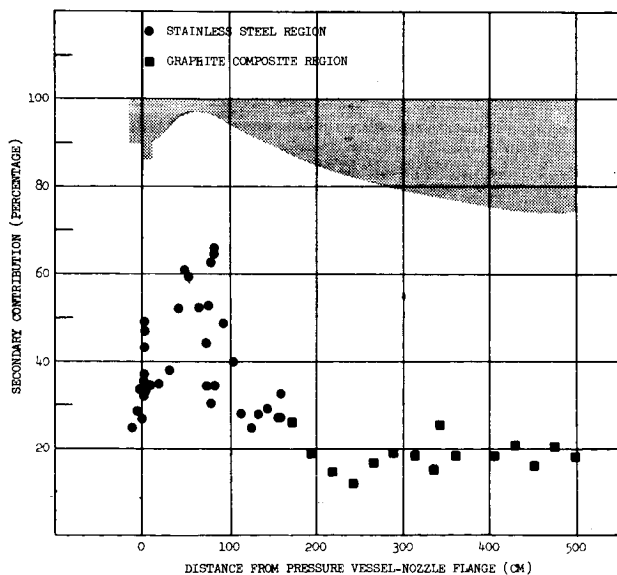


FIGURE 1  
NERVA Flight Engine Configuration

Gamma rays are far more effective than neutrons in heating metal components for the radiation leakages from NERVA. Typically, direct neutron interactions contribute about 4% of the total heating in the stainless steel nozzle. In the aluminum pressure vessel, fast neutrons contribute some 6% of the total heating opposite the core midplane. Neutrons must be considered not so much for their direct heating of metals, but because of their importance in producing secondary gamma radiation. Figure 2 presents the fraction of gamma heating in the nozzle due to secondary gammas produced in the nozzle assembly. Direct neutron heating is significant in only two components, the graphite nozzle extension and parts of the disk shield.

Heating rates in engine components presented in this paper are appropriate for the flight environment. During ground tests, additional radiation heating occurs in some components due to contributions from facility-related sources and facility scatter.<sup>2</sup> The components forward of the pressure vessel are designed to take advantage of the protection afforded by the internal shield in the flight environment. Special facility shielding is required to assure that these components are not overexposed in ground tests.

FIGURE 2



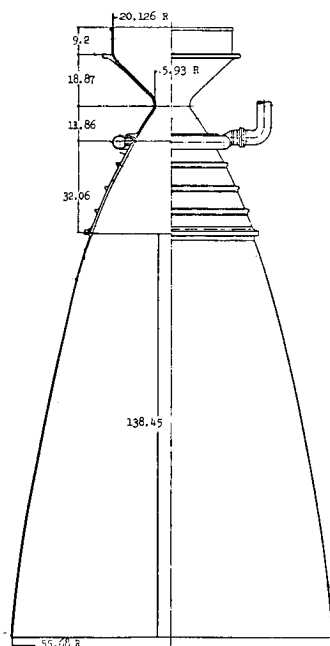
Flight environment heating rates are calculated in detail throughout the engine system using a variety of techniques. Coupled discrete ordinates-Monte Carlo techniques are used extensively. The DASH coupling code<sup>3</sup> has been used to bridge DOT<sup>4</sup> with COHORT<sup>5</sup> for calculations of the nozzle radiation environment and bridge DOT with DOT to calculate heating within the disk shield. Extensive point kernel calculations are used to check the predictions of the more sophisticated methods. Also, the point kernel codes, QAD<sup>6</sup> and GGG<sup>7</sup>, are used to predict the facility perturbation of the ground test environment. Calculated volumetric heating rates are input to thermal analyses. Predicted temperatures are necessary for subsequent stress and reliability analyses of candidate component designs.

A numerical differencing code, CINDA<sup>8</sup>, is used to predict temperatures throughout the components. It is used to construct and analyze mathematical models of any arbitrary one-, two-, or three-dimensional representation of physical systems governed by the Fourier equation with a source term. The user constructs a thermal analog network representing the system of interest. Non-linear material properties and boundary conditions may be simultaneously calculated as a function of one or more independent variables. For cooled components (e.g., the nozzle), CINDA is used to calculate the steady-state temperatures using the full power heating rates. For uncooled components (e.g., the disk shield), a transient analysis is conducted to yield the temperature as a function of time.

Before the individual components are considered, it should be emphasized that the NERVA flight engine design is in the preliminary design stage. Both the engine layout and the design of individual components, hence, the heating rates, have been revised periodically. However, the techniques used to calculate radiation heating and resulting temperatures can be applied to any configuration and every attempt is made to simplify the analyses required. The particular components and data presented in this paper were selected to illustrate the analytical approach to radiation heating in the NERVA engine.

One of the most important components in the engine is the nozzle assembly. It consists of a metal primary nozzle with a graphite extension as shown in Figure 3. Currently the candidate primary nozzle materials are CRES-347 stainless steel, Hastelloy X, and ARMCO 22-13-5. The nozzle extension is to be fabricated from a fibrous reinforced graphite composite material. Because of the intense gamma heating and consequent temperature increases, the decrease in allowable stress at the convergent cone section is a major design constraint. Therefore, the primary nozzle must be cooled with a portion of the LH<sub>2</sub> flow from the pump discharge line. Sufficient coolant flow must be provided to assure that the bulk steel temperature is maintained below about 1050°F. Not only is gamma heating an important internal volumetric source, but the hot exhaust gases (4000°R) flow over the inside surface of the nozzle hydrogen coolant tubes. Total nuclear heating rates in the primary nozzle shown vary from 0.6 BTU/in<sup>3</sup>-sec in the core support barrel to 0.01 BTU/in<sup>3</sup>-sec near the nozzle extension interface. The neutron contribution is only about 4% of the total heating in the steel. For these rates, the temperatures attained in the nozzle vary from -300°F in the coolant passages to a maximum of 900°F in the nozzle wall for the designs currently under consideration.

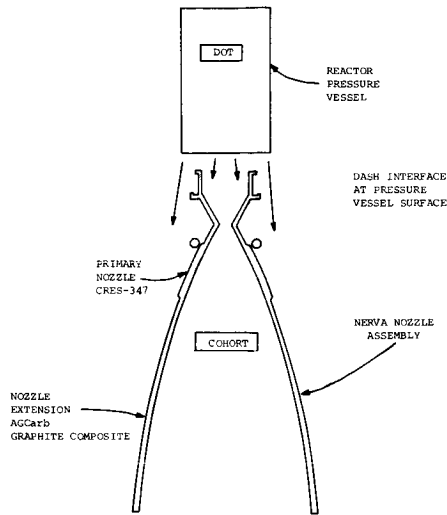
Figure 3  
THRUST CHAMBER ASSEMBLY  
FOR  
MONTE CARLO ANALYSIS



In the graphite nozzle extension, the total heating rates range from 0.002 to 0.0002 BTU/in<sup>3</sup>-sec, with the fast neutron heating contributing about 40% to the total. The graphite composite nozzle extension is only radiatively cooled since it can tolerate higher temperatures than metals (above 3000°F) and is subjected to lower heating rates. After 60 minutes of continuous full power operation, the temperature of the graphite varies between 1850°F and 2650°F.<sup>9</sup>

The calculational technique used to generate steady-state nuclear heating rates is shown in Figure 4. A DOT two-dimensional discrete ordinates transport code produces a leakage tape for the lower part of the pressure vessel and reactor assembly. The DASH single event Monte Carlo coupling code is used to transport this radiation across the void between the DOT source tape and the nozzle. The COHORT Monte Carlo code is used to calculate the radiation environment throughout the nozzle assembly.<sup>10</sup> Subsequently, CINDA is used to calculate the temperatures in the nozzle and nozzle extension.

Next consider the results for the pressure vessel. This component consists of an Al-7075 barrel and an Al-6061 dome. The dome is attached to the barrel by a forward closure flange with 124 bolts of A-286 alloy. Peak heating rates in aluminum opposite core midplane range from about 0.26 BTU/in<sup>3</sup>-sec on the inside surface to 0.18 BTU/in<sup>3</sup>-sec on the outside surface. In spite of these high volumetric heating rates, the coolant flow keeps the peak wall temperature in the pressure vessel below 100°F. The temperatures attained are strongly influenced by the coolant flow allocated to the reflector region. Most of the pressure vessel steady-state temperatures are below 0°F for the current flow conditions. In the top closure flange, high density A-286 bolts attain higher temperatures than the surrounding aluminum. Typically the aluminum in the flange is about -160°F, with the bolt 13°F higher since the gamma heating rates in the bolt are about a factor of three higher than in the aluminum. To prevent fluid leakage at this closure, the bolts are prestressed upon assembly of the pressure vessel.



MODEL FOR CALCULATION OF THE RADIATION ENVIRONMENT  
NERVA NOZZLE ASSEMBLY

Figure 4

The lower portion of the thrust structure is an aluminum cylindrical annulus with an inside radius of 19 inches and a thickness of 0.28 inches. It is attached directly to the pressure vessel. Not only does this structure transmit the thrust developed by the engine to the rest of the vehicle, but it supports part of the propellant feed system. If possible, the thrust structure should be designed so that it requires no coolant to keep temperatures below the allowable design limits. Currently two materials are under consideration for this component. The primary design uses aluminum which is limited to a maximum temperature of 300°F because above that temperature age hardening is gradually lost. An alternate design uses titanium which is limited to 700°F by the decrease in the yield stress with increasing temperature. Both designs are protected to a large extent by the shadow shield inside the pressure vessel. Heating rates in aluminum range from  $3 \times 10^{-3}$  BTU/in<sup>3</sup>-sec in the lower thrust structure near the pressure vessel dome to about  $5 \times 10^{-4}$  BTU/in<sup>3</sup>-sec in the upper thrust structure near the propellant tank. Peak temperature rises in the lower thrust structure are on the order of 200°F or less for an engine without a disk shield.

Since the thrust structure is uncooled, the temperature attained after a period of full power firing is strongly influenced by the initial temperature. Coatings such as Al<sub>2</sub>O<sub>3</sub> can be used to keep the initial temperature below 100°F. If the thrust structure must be cooled, it will impact on the engine and introduce additional failure modes. An uncooled thrust structure design is thus favored to increase the reliability of the engine design.

The disk shield shown in Figure 5 may be required for some manned missions with light payloads. It is designed to operate as an uncooled component. Such a design permits the use of a single NERVA engine for any manned or unmanned mission. If a light payload requires additional personnel shielding, a disk shield may be added to the engine with a minimum impact on the total engine design.<sup>11</sup> The largest shield design considered (shown in Figure 5) is a 10,000 lb disk with regions of stainless steel, lead, borated graphite, and lithium hydride.

#### EXTERNAL ENGINE DISK SHIELD

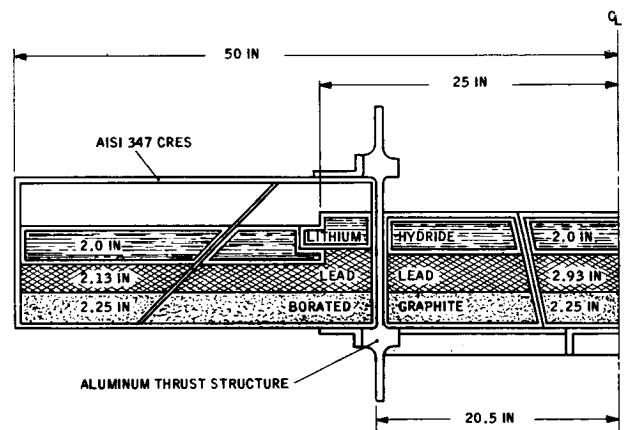


FIGURE 5

Table 1 presents the specification extreme heating rates in various regions of the shield. Neutron heating from the  $^{10}\text{B}(n,\alpha)^7\text{Li}$  reaction is the most important source in the borated graphite. Only gamma heating is of significance in the lead. In lithium hydride the  $^6\text{Li}(n,\alpha)^3\text{H}$  reaction is the most important source of heating. Fast neutron reactions are second in importance, followed by small values of gamma heating. Heating is much higher in the periphery of the shield since leakage radiation from the sides of the PVARA can "view" the disk around the internal shield.

Table 2 presents the peak temperatures for specification extreme (worst case) nuclear and thermal analyses in the disk shield for continuous firing times of 10, 30, and 60 minutes. The peak temperatures occur at the tip of the shield and decrease with decreasing radius. If some conservatism is removed by the use of nominal instead of "worst case" values for some parameters, the temperatures are lowered by at least  $150^\circ\text{F}$ . For instance, the lead at the outer edge of the shield remains below  $600^\circ\text{F}$ . Design options can also be exercised to circumvent thermal problems. For example, if the temperature is excessive in the lithium hydride, it can be removed from the outer 10 inches of the periphery of the shield.

The initial temperature of the disk is an important parameter in these calculations. It is expected that coatings such as aluminum oxide will assure that the initial temperature will not differ significantly from the ambient temperature at launch, even after a long space soak. Note that in Table 2 the initial temperatures differ in the central and peripheral portions of the shield. This is because the central portion is enclosed by the lower thrust structure and is inhibited from losing heat by radiation.

The heating rates in uncooled components near the bottom of the propellant tank, such as the gimbal assembly and the gimbal actuator, are about  $1.5 \times 10^{-3}$  BTU/in<sup>3</sup>-sec in steel. The aluminum upper thrust structure is subjected to heating rates on the order of  $5.5 \times 10^{-4}$  BTU/in<sup>3</sup>-sec in aluminum. For these low rates the gimbal temperature may increase  $250^\circ\text{F}$ , and the upper thrust structure temperature may increase by  $70^\circ\text{F}$  after 60 minutes of full power firing. Thus, radiation heating is not a factor in the design of such components.

#### REFERENCES

1. WARMAN, E. A., ROGERS, D. R., COURTNEY, J. C., DIXON, C. D., SMITH, J. R., and CONANT, J.: "Radiation Exposure Limitations for Shielded NERVA Engine Components," Aerojet Nuclear Systems Company Report RN-S-0557, April 1970.
2. WARMAN, E. A., FOREMAN, D. L., and COURTNEY, J. C.: "Comparison of Computed and Measured Radiation Levels in NERVA Development Engine Tests," Trans. Am. Nuc. Soc., 12, 416 (1969).
3. LINDSTROM, D.G. and PRICE, J. H.: "Coupled Discrete Ordinates - Monte Carlo Technique and Applications to NERVA," Trans. Am. Nuc. Soc., 12, 952 (1969).
4. MYNATT, F. R., "A Users Manual for DOT, a Two-Dimensional Discrete Ordinates Transport Code with Anisotropic Scattering," Union Carbide Corporation, Nuclear Division, Report K-1694 (1967).
5. COLLINS, D. G. and WELLS, M. B., "COHORT - A Monte Carlo Program for Calculating Radiation Heating and Transport," Radiation Research Associates, Inc., Report RRA-T62 (1966).
6. MALENFANT, R. E., "QAD: A Series of Point-Kernel General-Purpose Shielding Programs," Los Alamos Scientific Laboratory Report LA-3573 (1967).
7. MALENFANT, R. E., RSIC Code Package CCC-75, Radiation Shielding Information Center, Oak Ridge National Laboratory.
8. LEWIS, D. R., GASKI, J. D., and THOMPSON, L. R., "CINDA-3G-Chrysler Improved Numerical Differencing Analyzer for 3rd Generation Computers," Chrysler Corporation Space Division, Technical Note AP-67-287 (1968).
9. Thermal and Fluid Flow Analysis Report, NERVA Program, Data Item S-31, Aerojet Nuclear Systems Company Report S-031-CPO90290-F1 (1970).
10. WARKENTIN, J. K. and COURTNEY, J. C., "Monte Carlo Radiation Transport Analyses of the NERVA Nozzle Assembly," Trans. Am. Nuc. Soc., 13, 439 (1970).
11. WARMAN, E. A., COURTNEY, J. C., and KOEBBERLING, K. O., "Final Report of Shield System Trade Study," Aerojet Nuclear Systems Company Report SO54-023, July 1970.

TABLE 1

Disk Shield Heating Rates  
Nuclear Heating Rate (BTU/sec)

	<u>Gammas</u> <u>(From Nuclear Subsystem)</u>	<u>Shield</u> <u>Secondaries</u>	<u>Neutron</u> <u>Absorption</u>	<u>Totals</u>
<u>Central Region</u>				
0 to 25 inch Radius				
Lower Steel Plate	1.4	0.1	0	1.5
Borated Graphite	2.1	0.1	2.0	4.2
Lead	4.3	0.3	0	4.6
Lithium Hydride	<u>0</u>	<u>0</u>	<u>4.1</u>	<u>4.1</u>
	7.8	0.5	6.1	14.4
<u>Peripheral Region</u>				
25 to 50 inch Radius				
Lower Steel Plate	7.0	1.2	0	8.2
Borated Graphite	10.6	2.2	15.5	28.3
Lead	19.6	3.1	0	22.7
Lithium Hydride	<u>0.2</u>	<u>0</u>	<u>14.2</u>	<u>14.4</u>
	37.4	6.5	29.7	73.6
Shield Totals	45.2	7.0	35.8	88.0

TABLE 2

Disk Shield Peak Temperatures

<u>Material Regions</u>	<u>Initial</u> <u>Temperature</u> <u>in °F</u>	<u>Specification Extreme Peak Temperatures (°F)</u> <u>Time of Continuous Full Power Firing</u>		
		<u>10 Minutes</u>	<u>30 Minutes</u>	<u>60 Minutes</u>
<u>Central Region</u>				
Lower Steel Plate	100	160	252	330
Borated Graphite	100	156	248	325
Lead	100	154	245	320
Lithium Hydride	100	150	240	305
<u>Peripheral Region</u>				
Lower Steel Plate	70	350	630	870
Borated Graphite	70	280	540	780
Lead	70	260	520	760
Lithium Hydride	70	170	390	630